Submitted to Physical Review Special Topics: Accelerators and Beams, 1/21/2000

Simulations of a Multipactor-Inhibited Waveguide Geometry

Eric Chojnacki
Cornell University, Laboratory of Nuclear Studies, Ithaca, NY 14853

Studies of multipactor resonances in coaxial and hollow waveguide via standard particle trajectory and secondary emission numerical simulation techniques are presented. Agreement between simulations and experimentally observed multipactor barriers gives confidence in results of simulation studies of a wedge-shaped hollow waveguide geometry that shows promise of being far less susceptible to multipactor resonances than standard coax and hollow rectangular waveguides.
PACS Codes: 52.80.Vp, 52.80.Pi, 52.20.Dq

I. INTRODUCTION

Multipactor resonances in the waveguide feeding RF cavities often hinder coupling of RF power to particle beams. This is especially true in superconducting RF (SRF) cavities with characteristic long-pulse or CW operation, exacerbated by cold waveguide regions containing condensed gases which enhance the surface secondary emission coefficient. Previous numerical simulation studies of multipactor in waveguide have reported good agreement between simulated power barriers and those experimentally observed. Waveguide geometries studied have included the coaxial waveguide of the TESLA Test Facility (TTF) [1,2] and hollow rectangular waveguide of the Cornell Electron Storage Ring (CESR) [3]. This lends confidence to the predictive power of such simulation studies.

A clue to suppressing multipactor in waveguide is provided by the experience of suppressing many virulent multipactor resonances in cavities. This was accomplished over two decades ago by implementation of a rounded SRF cavity profile instead of pillbox [4]. Electron trajectory tracking codes subsequently quantified the benefits of a rounded cavity profile in regard to eliminating many multipactor resonances [5]. Thus, a similar geometrical approach to waveguide coupler variation is presented here. First, the salient features of a multipactor simulation code will be discussed. Results from the code will then be presented for familiar multipactor resonances in coaxial and hollow waveguide with particular attention to multipactor trajectory characteristics. Insight from these familiar resonances will then be used to propose a multipactor-inhibited wedge-shaped hollow waveguide geometry. The simulation code will then be applied to this "wedgeguide" and the promising results summarized.

II. MULTIPACTOR SIMULATION CODE

The simulation code utilized here employs many well known procedures for predicting multipactor resonances [6]. Electron trajectories were computed by fourth order Runge-Kutta solution of the full 3D Lorentz force equations. All electromagnetic fields for the cases in this study were single modes of axially uniform waveguide which were expressible in analytic form. Further, the modes were taken as simple CW traveling waves. Electrons were launched from a range of selected cross-sectional locations at a range of RF phases, typically from -30˚ to 180˚ in 5˚ steps with the electric field $E \propto \sin(\phi)$. RF power was scanned over a selected range in 1 kW steps. The initial electron and all secondaries were launched at an energy of 2 eV normal to the surface. The code typically runs for 20 impacts per initial launch condition, terminated if

secondary multiplication becomes $<10^{-3}$ or if the impacting electron energy is below some threshold, such as 0.1 eV. For each case of RF power level, launch phase, and launch location, secondary electron multiplication due to wall impacts is logged by a multiplicative counter utilizing a familiar curve of secondary electron yield vs. impact energy [7]. At each power level these secondary multiplications are summed over all launch phases. This is similar to what has been termed an "enhanced counter function," except there is no termination of the simulation decided by electric field polarity upon secondary launch [6].

Electron trajectories in multipactor simulations can be sensitive to numerical error due to the large number of integration time steps [8]. For the cases considered here with 500 MHz RF frequency and peak electric field of the order 100 kV/m, the optimal time step was found to be of the order 1 ps. Multipactor *resonant* trajectories were fairly tolerant to numerical error, yielding nearly identical results in regard to final trajectory position and secondary multiplication for time steps anywhere in the range 0.1-10 ps. *Non-resonant* trajectories were quite sensitive to numerical error, even occasionally showing false resonances that were elucidated by evaluation of accumulated error and trajectory reproducibility upon modest variation in time step.

III. COAXIAL AND HOLLOW RECTANGULAR WAVEGUIDE

As a test of the code described in Section II, it was run for known simulated and experimental cases of coaxial and rectangular waveguide. The results of secondary electron multiplication over a range of RF power are shown in Fig. 1 for TESLA 40 mm, 50 Ω coax driven at 1.3 GHz and in Fig. 2 for CESR 10.2 cm × 43.2 cm rectangular waveguide driven at 500 MHz. These agree well with previous simulations and experiments [2,3].

In rectangular waveguide, TE_{10} mode 2-point multipactor resonances occur between broadwalls along the cross-sectional midline at the peak of the electric field. Using the rectangular waveguide TE_{10} field convention of E_y, B_x, and B_z, these resonances have slow migration along the *z*-axis arising from the $v_y \times B_x$ Lorentz force. Interestingly, trajectories launched displaced from the midline experience a transverse $v_y \times B_z$ force and migrate to the sidewall after a few impacts, as shown in Fig. 3. There, the electric field is zero and magnetic field finite, thus successive cyclic low energy impacts quickly damp secondary multiplication to negligible levels. Even a small perturbation from the midline equilibrium, such as 1 mm, leads to migration to the sidewall, as shown in Fig. 4. This implies that a narrow strip along the center of rectangular waveguide is solely responsible for observed multipactor barriers. Though seemingly surprising, the barriers presented in Fig. 2 by such midline trajectories agree quite well with experiment.

For coaxial couplers with aligned, round conductors, troublesome multipactor resonances driven by the TEM mode typically occur with repeating impacts on the outer conductor. Trajectories closely follow the radial electric field and have slow migration along the axis arising from the $v_r \times B_\theta$ Lorentz force. Again, coax multipactor barrier power levels predicted by simulation agree well with experiment.

IV. WEDGEGUIDE

Since both rectangular and coaxial waveguide multipactor trajectories remain well aligned with the respective mode's electric field, a resonance-disrupting effect may be provided by altering the waveguide cross section so as to force a curvature on the electric field. This could disallow trajectories from traversing repeatable paths and even guide electrons to regions of zero electric field.

One such unconventional waveguide cross section is illustrated in Fig. 5. Rectangular waveguide is altered to have the broad walls non-parallel and the sidewalls as circular arcs to facilitate analysis. This "wedgeguide" has a lowest-cutoff mode similar to the rectangular TE_{10}. Modifications to coax have been explored elsewhere, but since TEM modes have no region of zero electric field and topology requires at least two places where inner and outer conductor surface normal vectors point at each other, resonant trajectories remained [9,10]. Discussion of the wedge-shaped hollow waveguide follows.

A. Wedgeguide Fundamental Mode

A MAFIA [11] solution of the electric field of the lowest-cutoff mode of the waveguide illustrated in Fig. 5 is shown in Fig. 6. This mode can be analytically treated in cylindrical coordinates as a higher order *TE* mode of coaxial waveguide [12]. The broad walls are on $\theta = const$ surfaces and the sidewalls are on $r = const$ surfaces, as indicated in Fig. 5 by the dimensions a, b, and α. The azimuthal harmonic of this *TE* mode is $n = 0$ and the cutoff wavenumber k_c is given by solution of the transcendental equation

$$\frac{J_o'(k_c a)}{J_o'(k_c b)} = \frac{N_o'(k_c a)}{N_o'(k_c b)} \quad , \tag{1}$$

where J_n and N_n are Bessel functions of the first and second kind, respectively. The field components are given by

$$E_\theta = E_o\left[J_1(k_c r) - gN_1(k_c r)\right]\mathrm{e}^{j(\omega t - \beta z)} \tag{2a}$$

$$H_r = \frac{-\beta E_\theta}{\omega\mu} \quad , \tag{2b}$$

$$H_z = \frac{-jk_c E_o}{\omega\mu}\left[J_0(k_c r) - gN_0(k_c r)\right]\mathrm{e}^{j(\omega t - \beta z)} \tag{2c}$$

where

$$g \equiv \frac{J_1(k_c a)}{N_1(k_c a)} \quad . \tag{3}$$

The peak azimuthal electric field occurs at a radius r_e solving

$$J_0(k_c r_e) - \frac{J_1(k_c r_e)}{k_c r_e} - g\left[N_0(k_c r_e) - \frac{N_1(k_c r_e)}{k_c r_e}\right] = 0 \tag{4}$$

and has the value

$$E_{\theta\ peak} = E_o\left[J_1(k_c r_e) - gN_1(k_c r_e)\right] \quad . \tag{5}$$

Integration of the Poynting vector gives the propagating power as

$$P = \frac{\alpha E_o^{\,2}\beta}{4\omega\mu}\left[r^2\left(R_1^{\,2}(k_c r) - R_0(k_c r)R_2(k_c r)\right)\right]_a^b \quad , \tag{6}$$

where

$$R_n(x) \equiv J_n(x) - gN_n(x) \quad . \tag{7}$$

These analytic forms allow greater accuracy and computation speed of electron trajectories than using, e.g., interpolation of MAFIA fields shown in Fig. 6.

B. Wedgeguide Multipactor Simulations

The traveling-wave RF fields in eq. (2) were used in the above described multipactor code. The wedgeguide dimensions were taken as a modification to the CESR 10.2 cm × 43.2 cm rectangular waveguide where one sidewall is effectively reduced to a 5.1 cm height and the other increased to 15.2 cm by having Fig. 5 dimensions of a = 21.6 cm, b = 64.8 cm, $\alpha = 13.2^{\circ}$, and again driven at 500 MHz.

Running simulations over comprehensive ranges of RF power, launch phase, and launch position in wedgeguide have revealed three characteristics of electron trajectories:

1) The great majority of trajectories alternately impact on the broadwalls and quickly become anti-resonant with the RF. After a dozen or so impacts the accumulated secondaries perform successive low energy impacts and secondary multiplication quickly decays to negligible values.

2) Trajectories have a migration bias toward the larger radius sidewall due to the E_θ field curvature. Trajectories that survive anti-resonant conditions well enough to maintain a significant secondary multiplication typically migrate to this wall. There, the vanishing electric and finite magnetic fields allow only successive cyclic low energy impacts that quickly damp secondary multiplication to negligible levels, analogous to trajectories displaced from the midline in normal rectangular waveguide.

3) The outward radial migration due to the E_θ field curvature opposes the net inward radial $v_\theta \times B_z$ force that occurs at radii less than the peak of the E_θ field as given by eq. (4). For a range of trajectory radii there are specific RF power levels at which these opposing forces almost balance, and the electrons can remain close to resonant in an $r = const$ vicinity. Fortunately, the force balance is not constant along the trajectory nor on average, and electrons eventually becomes anti-resonant and/or migrate to a sidewall after a few dozen impacts, as shown in Fig. 7. The secondary multiplication function may be high upon arrival at the sidewall, but the vanishing electric and finite magnetic field there causes successive cyclic low energy impacts that quickly damp secondary multiplication to negligible levels.

Thus, among the multitude of power, launch phase, and launch position cases simulated for multipactor resonance in wedgeguide, none have exhibited a resonance which would present a multipactor power barrier. An illustration of this is shown in Fig. 8 where secondary multiplication vs. RF power in wedgeguide is plotted for initial electron launch at a radius of 29 cm per the lower axis in Fig. 7. (Launches at 29 cm have shown the greatest likelihood of exhibiting short term balanced trajectories described in item 3 above.) Secondary multiplication in wedgeguide for electron launch radii from 25 cm to 42 cm scanned in 0.5 cm steps is quite similar to Fig. 8, having values at all powers considerably less than unity. This is in sharp contrast to rectangular and coaxial

waveguide having numerous resonant secondary multiplications of over 10^4 after 20 impacts, as shown in Figs. 1 and 2.

V. CONCLUSIONS

Electron trajectory simulations show the "wedgeguide" waveguide geometry to be promising in having greatly reduced multipactor susceptibility. From an operational point of view, a waveguide coupler fabricated with this shape would still likely require processing to burn off emitters and "scrub" the waveguide surfaces. But it is hoped that such processing will proceed quickly and not show degradation as experienced with current cryogenic couplers. Care would also have to be taken to ensure there are a minimum of other multipactor-susceptible components in the coupler chain, such as developing a novel vacuum window comprised of a familiar self-matched elliptical ceramic [13], but framed in wedgeguide.

VI. ACKNOWLEDGEMENTS

I am quite grateful for useful discussions with R.L. Geng, J. Knobloch, and H. Padamsee.

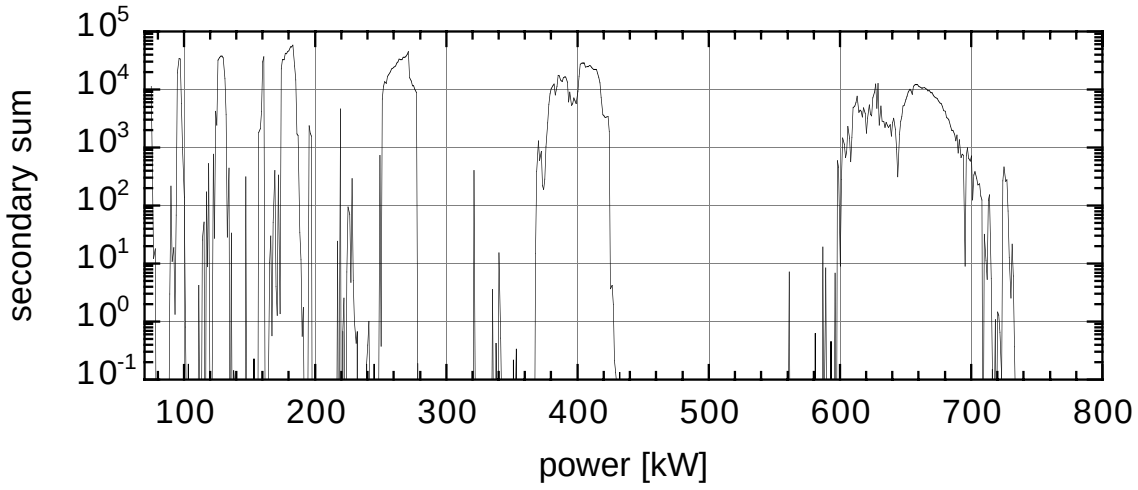

FIG. 1. Secondary multiplication summed over all launch phases in TESLA 40 mm, 50 Ω coax driven at 1.3 GHz with a maximum of 20 impacts.

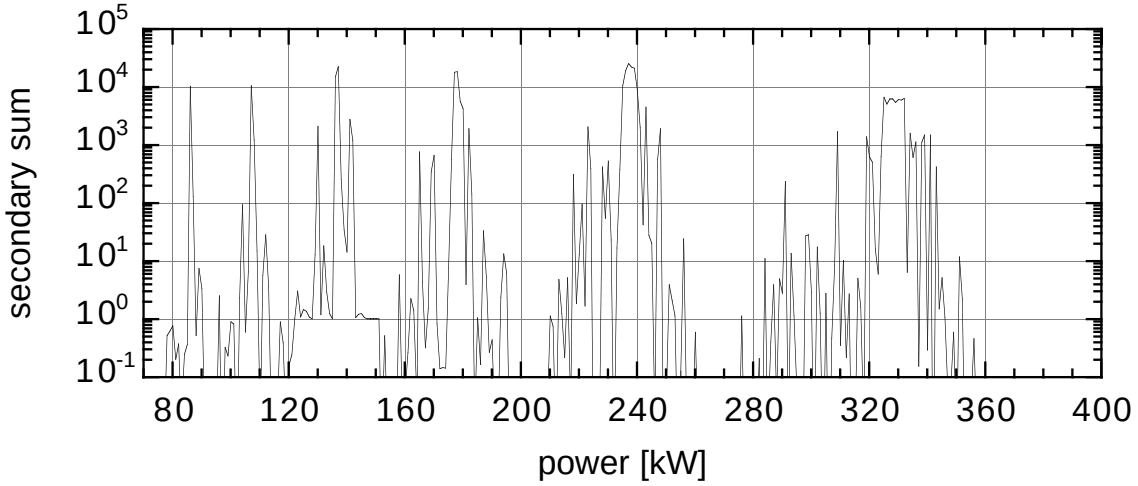

FIG. 2. Secondary multiplication summed over all launch phases CESR 10.2 cm × 43.1 cm rectangular waveguide driven at 500 MHz with a maximum of 20 impacts.

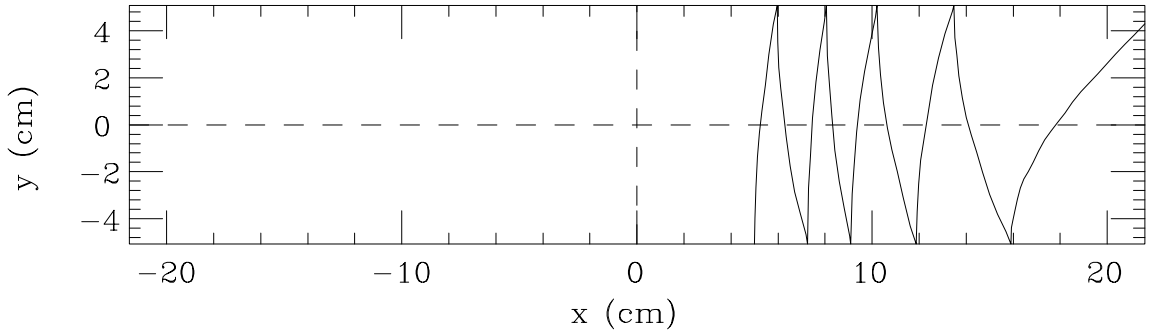

FIG. 3. Trajectory of an electron launched 5 cm from the midline in CESR rectangular waveguide propagating the TE_{10} mode.

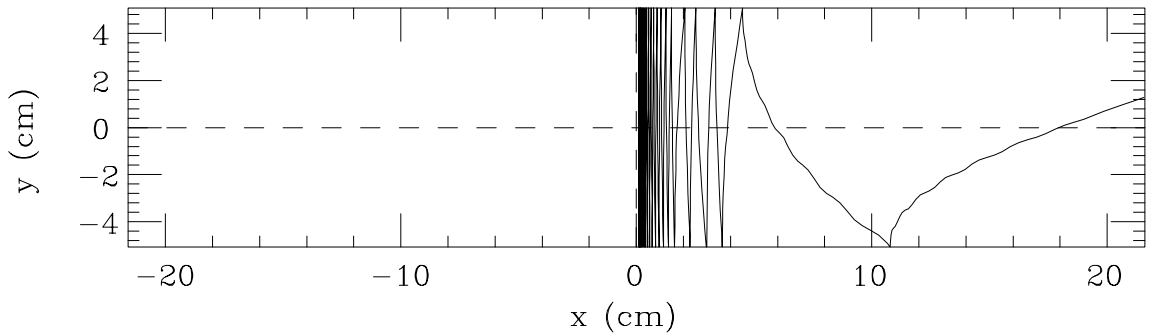

FIG. 4. Trajectory of an electron launched 1 mm from the midline in CESR rectangular waveguide propagating the TE_{10} mode.

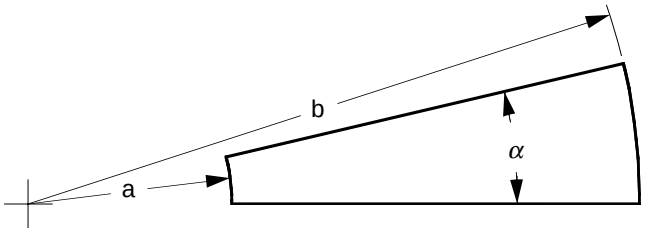

FIG. 5. Wedge-shaped cross section of a hollow waveguide.

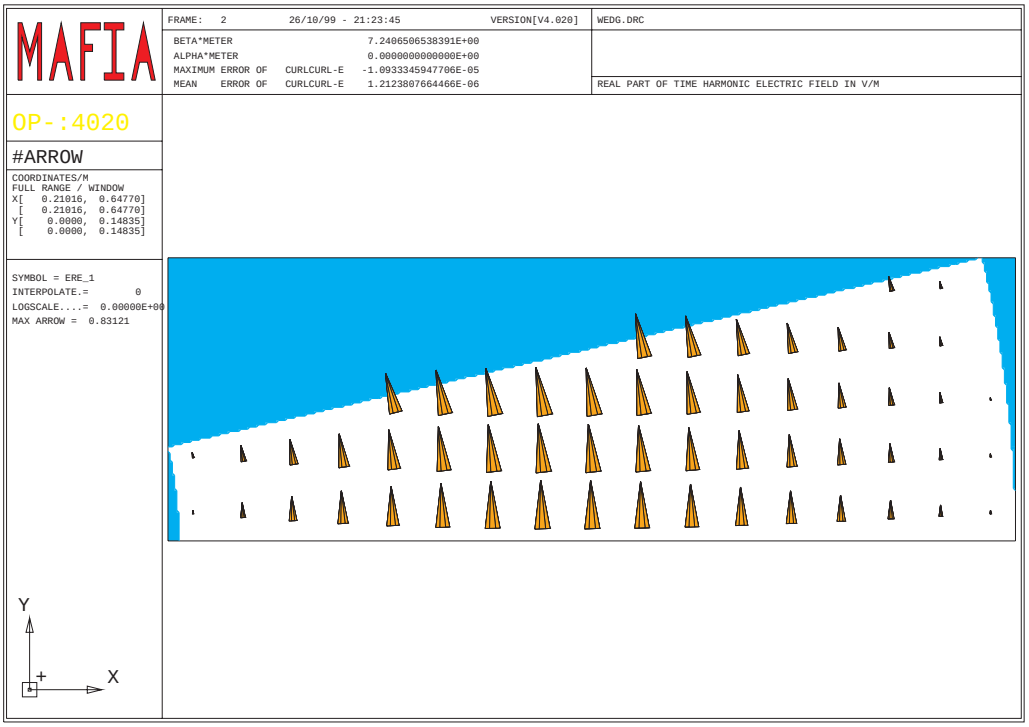

FIG. 6. MAFIA solution of the lowest-cutoff mode electric field in the wedge-shaped waveguide illustrated in Fig. 5.

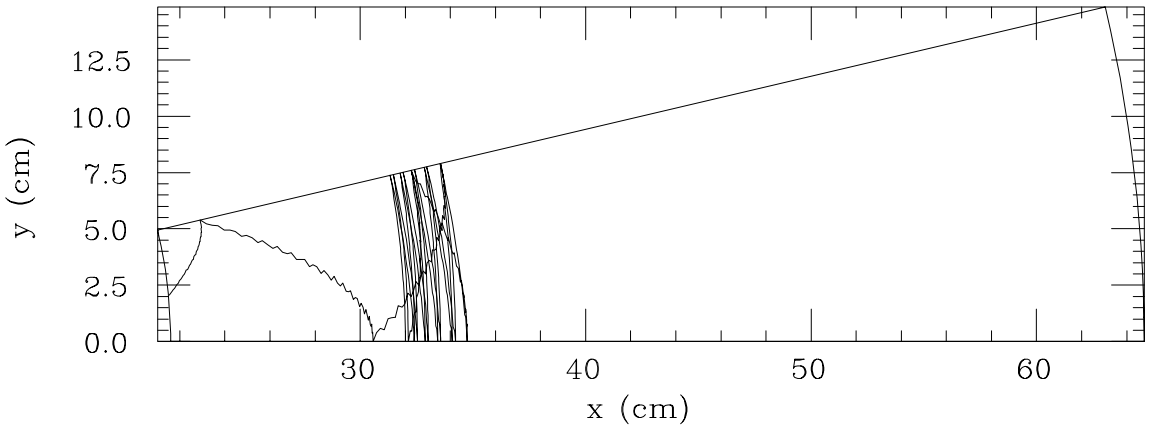

FIG. 7. Trajectory of an electron launched at a radius of 32 cm in wedgeguide and experiencing almost balanced transverse forces, eventually migrating to a sidewall.

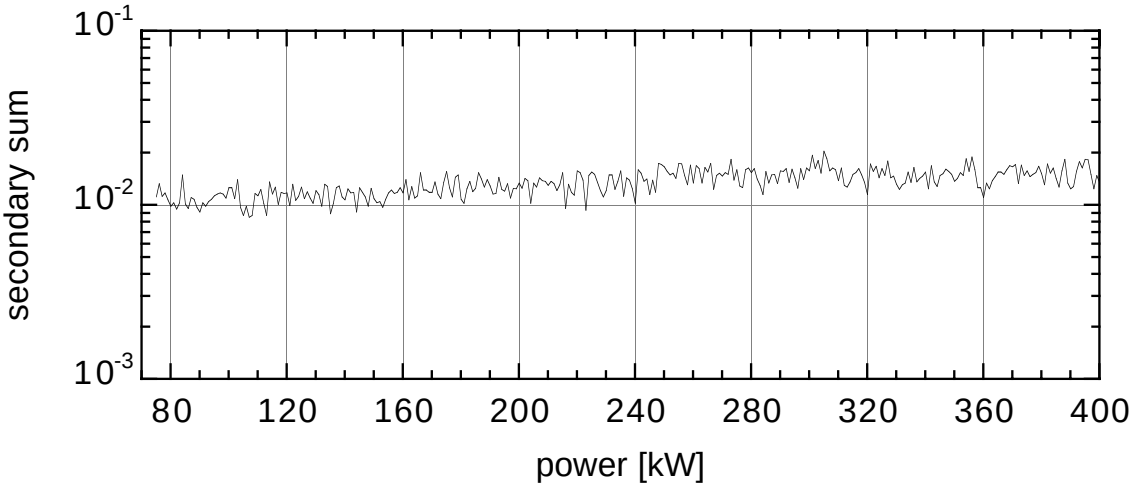

FIG. 8. Secondary multiplication summed over all launch phases in wedgeguide with dimensions a = 21.6 cm, b = 64.8 cm, $\alpha = 13.2^{\circ}$, driven at 500 MHz, and initial launch radius at 29 cm.

---

[1] E. Somersalo, P. Yla-Oijala, and D. Proch, in *Proceedings of the 1995 Particle Accelerator Conference, Dallas, TX*, edited by Laurie Gennari, (IEEE, Piscataway, NJ, 1996), p. 1500.

[2] B. Dwersteg, in *Proceedings of the 8th Workshop on RF Superconductivity*, 1997, edited by V. Palmierii and A. Lombardi,(LNL-INFN (Rep) 133/98, 1998), p. 740.

[3] R.L. Geng and H. Padamsee, in *Proceedings of the 1999 Particle Accelerator Conference, New York, NY*, edited by A. Luccio and W. MacKay, (IEEE, Piscataway, NJ, 1999), p. 429.

[4] V. Lagomarsino, G. Manuzio, R. Parodi, and R. Vaccarone, IEEE Trans. Magn. **MAG-15 (1)**, p. 25 (1979).

[5] U. Klein and D. Proch, in *Proceedings of the Conference on Future Possibilities for Electron Accelerators*, 1979, edited by J.S. McCarthy and R.R. Whitney, (U. Virginia, Charlottesville, VA, 1979), p. N1.

[6] E. Somersalo, P. Yla-Oijala, D. Proch, and J. Sarvas, Part. Accel. **59**, p. 107 (1998).

[7] H. Piel, in *Proceedings of the CERN Accelerator School: Superconductivity in Particle Accelerators, Haus Rissen, Hamburg, Fed. Rep. Germany,* 1988, edited by S. Turner, (CERN 89-04, Geneva, 1989), p. 176.

[8] W.H. Press, B.P. Flannery, S.A. Teukolsky, and W.T. Vetterling, *Numerical Recipes in Fortran 77: The Art of Scientific Computing* , (Cambridge University Press, Cambridge, 1996), 2nd Ed., **Vol. 1**, p. 708.

[9] J. Tuckmantel, CERN, LEP2 Note 94-25 (1994).

[10] J. Tuckmantel, in *Proceedings of the 1995 Particle Accelerator Conference, Dallas, TX*, edited by Laurie Gennari, (IEEE, Piscataway, NJ, 1996), p. 1642.

[11] Computer code MAFIA, CST-Gesellschaft fur Computer-Simulationstechnik mbH, www.cst.de.

[12] S. Ramo, J.R. Whinnery, and T. Van Duzer, *Fields and Waves in Communication Electronics*, (Wiley, New York, 1994), 3rd ed., p. 433.

[13] E. Chojnacki, T. Hays, J. Kirchgessner, H. Padamsee, M. Cole, and T. Schulteiss, in *Proceedings of the 1997 Particle Accelerator Conference, Vancouver, BC, Canada,* edited by M. Comyn, M.K. Craddock, M. Reiser, and J. Thomson, (IEEE, Piscataway, NJ, 1998), p. 3177.